Proceedings of the ICBBG2025
2025 International conference on Bio-mediated and Bio-inspired Geotechnics
18-20 May, 2025 | Tempe, Arizona, USA
https://doi.org/10.53243/ICBBG2025-120

Evaluation of System Compliance Issues in Laboratory Evaluation of Earthworm-Inspired Robotic Probes

Honglai Peng,[1] Rodrigo Borela,[2] and J. David Frost [3]

[1]Computational Science and Engineering, Georgia Institute of Technology, Atlanta; E-mail: hpeng73@gatech.edu

[2]School of Computing Instruction, Georgia Institute of Technology, Atlanta; E-mail: rborelav@gatech.edu

[3]School of Civil and Environmental Engineering, Georgia Institute of Technology, Atlanta; E-mail: david.frost@ce.gatech.edu

ABSTRACT

Traditional cone penetration tests (CPT) are indispensable for obtaining soil properties but come with limitations, including manual operation and an inherent restriction to vertical exploration. The remarkable ability of earthworms to navigate and manipulate soil environments with efficiency has inspired us to investigate this approach to soil exploration. Our research focuses on understanding challenges in designing a bio-inspired robotic system that autonomously navigates soil in multiple directions and enhances in-situ soil analysis while minimizing the soil disturbance. Our prototype device incorporates control systems including an MSP432 microcontroller and diverse actuation mechanisms, that enable optimal adaptability and precision within various soil conditions. In addition, by testing in different environments, including manufactured tubes and sandy soil conditions, it is possible to investigate the system robustness and adaptability. The refinement further enhances the system's interaction with soil, suggesting approaches to optimize its effectiveness. By investigating the ap- plication of bio-inspired robotics in geotechnical engineering, this work not only can enhance soil analysis techniques while reducing environmental impact, but also sup- port environmental research, infrastructure development, and disaster management.

INTRODUCTION

Soil exploration is a critical component in the field of geotechnical engineering, and is essential for understanding subsurface conditions to inform the design and construction of infrastructure. Traditional methods, such as Cone Penetration Testing (CPT), are generally limited to vertical probing in accessible areas. These limitations highlight the need for more advanced technologies capable of autonomous and multi-directional subsurface exploration.

To address these challenges, researchers have turned to bio-inspired robotic systems, getting inspiration from the efficient burrowing mechanisms of earthworms and other organisms, as stated in Martinez et al. 2022. Laschi et al. 2009 proposed a robotic arm design inspired by the arms

of octopus, capable of bending in all directions and achieving fast elongations. Lin, Leisk, and Trimmer 2011 investigated the advantages of morphing to enhance the locomotion speed of soft robots, inspired by the rolling motion of caterpillars. Kim et al. 2018 Lee, Lim, et al. 2019 Lee, Tirtawardhana, and Myung 2020 designed a rigid drilling robot drawing inspirations from the behaviors of mole rats, which use cutting, removal, and balancing to navigate in the subsurface. Kubota et al. 2007 Heung, Chiu, and Li 2016 Calderón et al. 2016 Kamata et al. 2018 and Das et al. n.d. 2023 focused on the development of peristaltic crawling robots inspired by earthworms to move in narrow space. Huang and Tao 2020 Chen, Khosravi, Martinez, and DeJong 2021 Chen and Martinez 2022 Zhang et al. 2023 and Chen, Martinez, and DeJong 2024 explored the self-burrowing mechanism inspired by razor clams using DEM simulations to optimize the interaction between the probe and soil, demonstrating the feasibility of efficient penetration strategies. Niu et al. 2015 and Luo et al. 2016 created scissor-lift structures that mimic the muscle functions of earthworms, enabling more efficient movement in confined environments. Borela 2021 Borela et al. 2021 developed a soft robotic system in our lab, utilizing the soil response to the anchor-push mechanism, inspired by the burrowing behavior of earthworms. These bio-inspired systems emulate the natural movement and soil interaction strategies of these organisms, leading to more versatile and adaptable tools for soil exploration.

Despite these advancements, overcoming the high soil resistance still remains challenging. Current robotic systems often struggle to penetrate the soil efficiently, particularly in denser conditions, where excessive resistance limits their effectiveness and scalability Borela et al. 2021 Chen, Khosravi, Martinez, and DeJong 2021 Chen, Khosravi, Martinez, DeJong, and Wilson 2020. This challenge underscores the need for more refined control mechanisms and feedback systems that can adapt to the dynamic and varied nature of subsurface environments. To address these limitations, we developed a new control system for the soft robot (SoRo) that leverages a microcontroller unit for precise control and real-time feedback. In this manuscript, we present the following contributions:

- We integrate the MSP432 microcontroller and diverse actuation mechanisms to ensure precise control and adaptability across various simulated subsurface conditions.
- We conduct testing of the system in different environments under various conditions, including tube and sandy conditions, to demonstrate its robustness and environmental adaptability.
- We provide insights into soil-robot interactions, offering a nuanced understanding of soil resistance which aims to advance geotechnical engineering techniques.

In section 2, we introduce our upgraded microcontroller unit control system, which builds upon the foundational work of Borela 2021 developed in our lab. This section details the enhancements made to improve the precision and adaptability of the SoRo system. Then, we describe our experimental setup and results, including tests conducted without soil and tests performed in soil, in sections 3 and 4, respectively. Finally, in section 5, we summarize our findings, discuss their implications, and propose directions for future research.

EARTHWORM-INSPIRED ROBOTICS CONTROL SYSTEM

The complete setup of our earthworm-inspired soft robot (SoRo) system is shown in Fig. 1. It is composed of three main subsystems: the microcontroller unit (MCU), the actuation subsystem, and the sensing subsystem, as illustrated in Fig. 2. The sensing subsystem comprises two 26PC-CFH6G pressure sensors to detect syringe pressure and two LM741 op-amps to amplify the signals.

These signals are processed by the MSP432P401R microcontroller from Texas Instruments (TI) in the control unit via its Analog-to-Digital Converter (ADC), which sends control signals to the DRV8825 motor drivers in the actuation subsystem. The motor drivers then control the stepper motors to push and pull the syringes, facilitating the expansion and contraction of the SoRo. In our research, we have specifically focused on enhancing the central control unit by integrating the microcontroller to improve the overall evaluation and precision of the system's functionality, while the remaining components follow the original configuration detailed in Borela 2021.

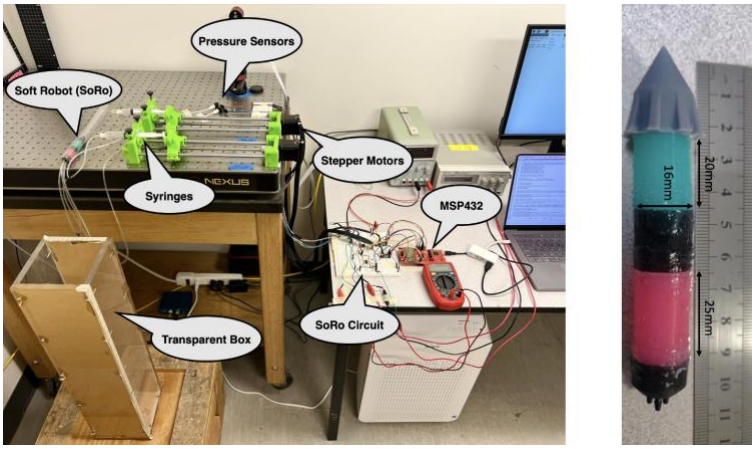

Figure 1: The overview of our soft robot system and the dimensions of the probe.

The SoRo probe, as shown in Fig. 1, consists of two main components: the Anchor and the Pusher. The Anchor (red component), made of soft materials, measures 25 mm in length and is responsible for creating anchorage when expanded by increased pressure. The Pusher (blue component), made of stiffer materials, measures 20 mm in length and facilitates forward movement by pushing the SoRo after the anchor has gripped the environment. The diameter of the SoRo is 16 mm. These components work together to mimic earthworm locomotion, enabling efficient movement through soil environments.

1. Microcontroller Unit In our microcontroller unit, we have selected the MSP432P401R to improve the precision of actuation control. This mixed-signal microcontroller operates at a 48 MHz clock speed, providing a balance between computational performance and power efficiency. It also features a 14-bit ADC for high-resolution signal processing and 78 GPIO ports, enabling extensive integration with multiple devices. Additionally, it is supported by robust development environments and various online resources, promoting easier development and debugging.

2. Actuation Subsystem The actuation subsystem is composed of stepper motor 17HD48002, motor driver DRV8825, linear stage platform and two syringe pumps, unchanged as in Borela 2021.

Stepper Motor The 17HD48002 stepper motor, developed by BUSHENG Motor, with a resolution of 200 steps/revolution, a holding torque of 0.59 Nm, a maximum push force of 25 N, and a rated current of 1.7 A, offers low cost and sufficient torque capacity for our system.

Motor Driver The DRV8825 is a motor driver designed for precise stepper motor control, compatible with both 3.3 V and 5 V systems, making it suitable for the MSP432P401R. It supports multiple step resolutions, from full-step to 1/32-step, enabling fine motion control. For example, in full-step mode, the motor completes 200 steps per revolution, while in 1/8-step mode, it achieves 1600 steps per revolution for finer resolution. Additionally, the DRV8825 is equipped with several safety features such as over-temperature, over-current, and under-voltage protection.

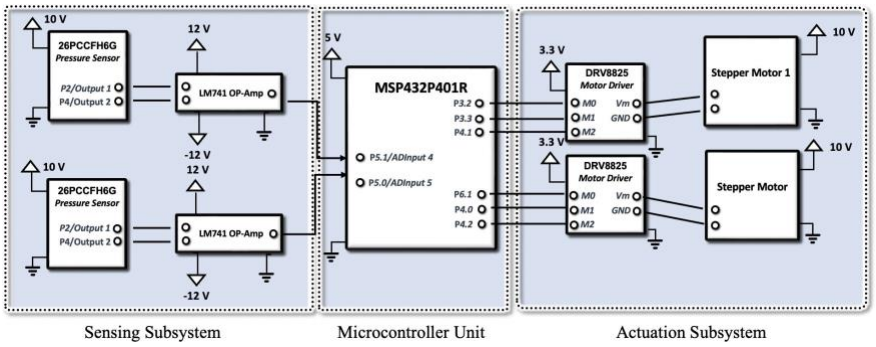

Figure 2: The overview of our soft robot system and the dimensions of the probe.

3. Sensing Subsystem The sensing subsystem consists of the pressure sensor 26PCCFH6G and the operational amplifier LM741.

Pressure Sensor The pressure sensor, developed by Honeywell Sensing and Control, operates within a 15 psi range and requires a 10 V supply voltage, ensuring compatibility with other system components. With a sensitivity of 6.67 mV/psi, it effectively detects pressure changes. Additionally, its robust sealing allows reliable operation in both air and water environments, making it suitable for our actuators. The pressure sensors remain the same as the one used in Borela 2021.

Operational Amplifier The LM741 series, developed by TI, are general-purpose operational amplifiers used to enhance signal processing in our lab-scale system. Given the low-pressure range of our selected sensor, the output voltage to the MSP432P401R remains in the millivolt range, making data collection and analysis challenging due to minimal voltage changes. Additionally, these low-voltage signals are highly susceptible to noise, further complicating experiments and evaluations. To address these issues, the LM741 effectively amplify the signals and improve the accuracy of our measurements.

FUNCTION EXPERIMENTS WITHOUGH SOIL

In this experiment, we evaluated two different actuator mechanisms, pneumatic and hydraulic, in the functional test without soil. Additionally, we assessed the system stability using syringes of varying sizes. Given that our MCU and stepper motor allow control over speed and step size, we also evaluated stability across different speeds and step sizes. These comparisons will help determine the optimal actuator setup for our future in soil lab tests.

4. Step Size Evaluation As discussed in Section 2, the motor driver supports multiple step modes. Based on observations and Borela 2021, the 1/8-step and 1/16-step modes are well-suited for our system. Larger step modes, such as full-step, half-step, or 1/4-step, cause rapid injection into the system, leading to temporary deformation of the syringe and tubes, which delays the pressure increase and causes instability. On the other hand, the 1/32-step mode produces steps too small to generate sufficient torque for effective syringe movement. The 1/8-step and 1/16-step modes provide a balance by offering more precise control and sufficient torque without the obvious instability observed with larger steps.

5. Syringe Size Evaluation During our laboratory tests, we evaluated three types of syringes: 3.5 ml, 10 ml, and 100 ml. Initial assessments demonstrated that there existed compatibility issues between certain syringe sizes and actuator types.

In the case of the pneumatic actuator, the 3.5 ml syringe was ineffective. As we mentioned above, our SoRo system operates based on designated pressure thresholds for both the anchor and pusher components. The 3.5 ml syringe failed to generate sufficient air pressure to meet the thresholds, resulting in system stalling during operation.

In the case of the hydraulic actuator, the 100 ml syringe proved unsuitable for two main reasons. First, the rubber plunger in the 100 ml syringe generated substantial friction, which exceeded the torque capacity of our stepper motor, hindering its movement. Even when the motor managed to overcome this friction, the high resistance introduced significant oscillations, compromising system stability and performance. Second, we propose that the 100 ml syringe caused rapid water injection even with the same step size. This led to temporary deformation of the syringe and soft rubber tubes, expanding the volume and delaying the pressure increase. Once the components returned to their original shape, the pressure rose quickly, resulting in an overshoot. The need to withdraw water to correct this overshoot caused further oscillations in the system.

Given these observations, the 10 ml and 100 ml syringes will be used in the pneumatic actuator tests, while the 3.5 ml and 10 ml syringes will be tested in the hydraulic actuator.

6. Speed Evaluation We use Code Composer Studio (CCS), developed by TI, to control our system. In our tests, we evaluated different speeds in terms of *revolutions per minute* (*RPM*) as follows: 600 *RPM*, 375 *RPM*, 300 *RPM*, 250 *RPM* and 200 *RPM*.

7. Results and Discussion In our experimental results, the notation *Anchor*_10_*M*16 represents an Anchor setup with a 10 ml syringe using a stepper motor in 1/16 mode, while *Pusher*_10_*M*16 refers to a Pusher with 1/16 mode. As shown in Fig. 3a, we evaluated the performance of our SoRo

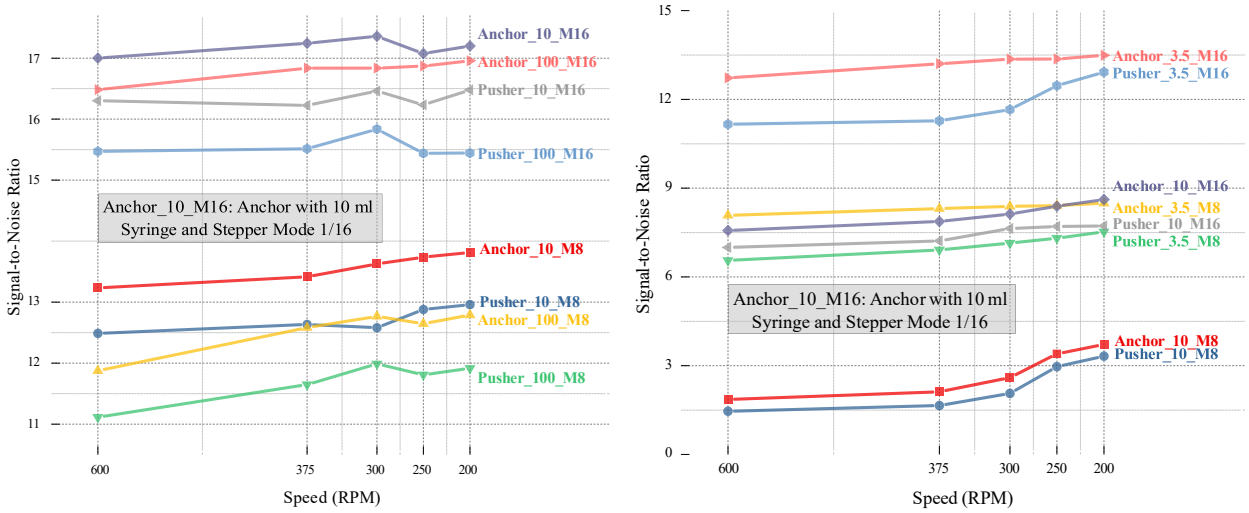

(a) (b)

Figure 3: (a) Experimental results of Signal-to-Noise Ratio (SNR) as a function of motor speed (RPM) to evaluate the pneumatic actuator performance with different syringe sizes and step modes.
(b) Experimental results of Signal-to-Noise Ratio (SNR) as a function of motor speed (RPM) to evaluate the hydraulic actuator performance with different syringe sizes and step modes.

system using a pneumatic actuator with various stepper modes, syringe sizes, and speeds. The performance is measured using the signal-to-noise ratio (SNR) (Johnson 2006), where a higher SNR

indicates better performance. The results demonstrate that 1/16-step mode outperforms 1/8-step mode. Additionally, within the 1/16-step mode plots, the *Anchor*_10_*M*16 configuration shows better performance compared to *Anchor*_100_*M*16 at any speed. Similarly, *Pusher*_10_*M*16 consistently achieves higher SNR values than *Pusher*_100_*M*16 across all speeds. Furthermore, the highest SNR is observed at a speed of 300 *RPM*.

As shown in Fig. 3b, we also evaluated the performance of our SoRo system using a hydraulic actuator with different stepper modes, syringe sizes, and speeds. The results show that, for both the anchor and pusher, the configuration with a 3.5 ml syringe and 1/16-step mode consistently performs the best compared to other settings. However, it is crucial to note that the SNRs achieved with all settings using the pneumatic actuator are higher than those obtained with the hydraulic actuator. As a result, we conclude that our SoRo system performs best with a 10 ml syringe and 1/16-step mode at a speed of 300 *RPMs* using pneumatic actuation.

It has been demonstrated that the SoRo system performed better with the 10 ml syringe compared to the 100 ml syringe in Fig. 3a. We propose that the 100 ml syringe introduced more friction due to the larger rubber perimeter of the syringe plunger, which increased the noise in our system. Additionally, as shown in both Fig. 3a and Fig. 3b, the 1/16-step mode consistently outperformed 1/8-step mode for both the pneumatic and hydraulic actuators. We propose that, in 1/8-step mode, the faster movement of the stepper motor leads to rapid air injection into the system, causing temporary deformation of the syringe and soft rubber tubes. This deformation results in a temporary expansion of the volume, delaying the pressure increase. As the components return to their original state, the pressure rises rapidly, leading to an overshoot of the pressure threshold. This overshoot requires the withdrawal of air, which subsequently causes oscillations in the system. Moreover, overshooting may risk exceeding the material capacity of the SoRo, potentially leading to permanent damage like leaks. Second, based on our observations, the stepper motor moved more smoothly in 1/16-step mode compared to 1/8-step mode. The smoother motion helped reduce the intermittent movements of the syringe caused by larger steps in 1/8-step mode, which could otherwise introduce instability and noise into the system. Moreover, we observe that the pneumatic actuator outperforms the hydraulic actuator. This can be due to the compressibility of air in the pneumatic system, which acts like an air tank. This helped to reduce oscillations, resulting in smoother control of the system. In contrast, the less compressible nature of the water in hydraulic actuators leads to more immediate transmission of forces, causing less smooth movements and increased oscillations.

FUNCTION EXPERIMENT WITHIN SOIL

As shown in Section 3, the pneumatic actuator outperformed the hydraulic actuator in lab-scale tests. Additionally, the 1/16-step mode combined with a speed of 300 *RPMs* proved to be the optimal configuration for our pneumatic actuator. We also evaluated our system within the soil, focusing on two key aspects: the effects of varying soil porosity and the influence of rigid walls.

1. Various Density Effects Test Our specimen chamber consists of a transparent box with dimensions of 30 cm in height, and 12 cm in both width and length. In our experiment, we used Ottawa sand as the testing material. To prepare the soil specimen with varying density levels, we utilize a stainless steel funnel.

During specimen preparation, we adjust the density by varying the height between the soil surface and the funnel opening. A larger height results in higher density (lower void ratio).

We conducted height adjustments at 2 cm, 15 cm, and 30 cm. The porosity calculations demonstrated that the porosity remained relatively constant between 15 cm and 30 cm, indicating that porosity did not change beyond 15 cm. As a result, we prepared specimens using the 2 cm and 15 cm heights. The 2 cm height produced a porosity of 0.38, corresponding to a void ratio of 0.61 and a relative density of 62.37%, while the 15 cm height yielded a porosity of 0.35, with a void ratio of 0.54 and a relative density of 87.18%. Based on the standard properties of Ottawa sand, which has a void ratio range of 0.50 to 0.80 (He and Chu 2014 A. Martinez et al. 2018), our experimental conditions are within the expected range. In all tests within this part of the study, the soft robot was positioned at the center of the specimen.

2. Various Rigid Wall Effects Test As shown in Fig. 4, we evaluated the effects of the rigid wall by adjusting the distance between the SoRo and the wall to 0 cm, 3 cm, and 6 cm, which is the midpoint of the specimen. Throughout the tests, the SoRo was consistently positioned at a height of 15 cm.

Figure 4: The image shows the process of preparing the specimen for testing the rigid wall effects, with a distance of 0 cm from the rigid wall. These configura- tions were also used when testing the effects of differ- ent porosities.

3. Results and Discussion As shown in Fig. 5a, *Edge_0_Porosity_0.35* denotes the condition where the specimen was prepared with porosity of 0.35, and a distance of 0 cm from the rigid wall. Also, the y-axis represents the volume of air injected into our SoRo, while the x-axis indicates the functions of the anchor and pusher.

For the anchor, less air volume is required to reach the target pressure when the soil porosity is lower. This indicates that lower porosity, which corresponds to higher relative soil density, exerts greater pressure on the SoRo, reducing the need for additional air. However, the air volume required for the pusher remains almost constant across different porosities. We propose that this is because the pusher's materials are stiffer than the anchor, making the pusher less responsive to the varying pressures exerted by the surrounding soil. Additionally, the volume of air required for different distances from the rigid wall remains nearly constant. We propose two reasons for this observation: First, the target pressure applied to our SoRo might not be high enough to cause substantial deformation, making the effects of the rigid wall less noticeable. Second, although the rigid wall does affect the SoRo, the small size of the specimen means that even the maximum distance of 6 cm from the wall is insufficient to significantly mitigate its effects, making it challenging to observe clear differences.

To better understand the interactions between soil and SoRo, we plotted a series of anchor and pusher functions, as shown in Fig. 5b. The observations indicate that pressure changed more rapidly during anchor contraction than expansion. When the anchor expands, it pushes the surrounding sand away, shearing the soil and displacing it outward. During contraction, since our target pressure was not high enough to induce sufficient deformation, and the friction

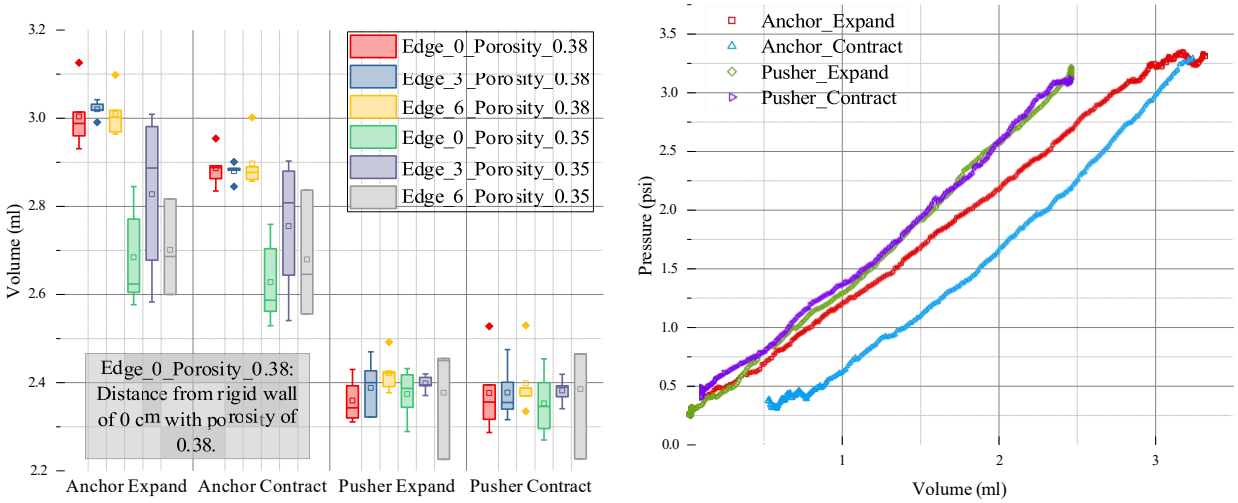

(a) (b)

Figure 5: (a) Experimental results of the injected volume (ml) for anchor and pusher under dif- ferent conditions, including two porosity levels (0.35 and 0.38) and three distances from the rigid wall (0 cm, 3 cm, and 6 cm). (b) Pressure-volume relationship for anchor and pusher operations, showing interactions between soil and SoRo components (anchor and pusher) during expansion and contraction phases.

between sand particles was substantial enough to prevent collapsing, the opposing pressure from the soil was lower compared to expansion. This discrepancy is reflected in the observed pressure coefficients, with anchor expansion at approximately 0.9 and contraction at 1.4, indicating a faster pressure drop during contraction. The increased volume of the anchor at the same pressure during contraction further supports the reduced opposing resistance from the surrounding soil. A similar effect of volume on penetration resistance was observed in earthworm-inspired probes, where varying inflation volume influenced penetration behavior (Naziri et al. 2024). Moreover, the pusher exhibited similar pressure coefficients for expansion and contraction, around 1.0, likely due to its stiffer materials minimizing deformation and reducing soil pressure effects.

CONCLUSION AND FUTURE RESEARCH

This study presents the development and preliminary evaluation of an earthworm-inspired soft robotic test system designed for advanced soil exploration, with a focus on achieving precise control through the use of a microcontroller unit. The experimental results demonstrate that the performance of the SoRo system is influenced by syringe size, stepper mode, and actuator type. Specifically, the 10 ml syringe, in combination with the 1/16-step mode and pneumatic actuator, consistently yielded the highest signal-to-noise ratios, showcasing the precise control and stability of our system.

In these lab-scale tests, the pneumatic actuator outperformed the hydraulic actuator, primarily due to the compressibility of air, which provided a damping effect that reduced oscillations and enabled smoother, more controlled movements. Our study also revealed that different soil densities affect system performance: higher density required less air volume for the anchor to reach target pressure. However, the pusher's performance remained relatively consistent across different

porosities, due to its stiffer materials that minimized deformation under pressure of the surrounding soil. Regarding rigid wall effects, minimal impact was observed, due to the limited size of the test specimen and insufficient target pressure to induce enough deformations.

Our future work will focus on exploring rigid wall effects more comprehensively using larger specimens, which should provide deeper insights into boundary interactions and their influence on SoRo performance. Additionally, we plan to upscale our experiments to test the system in larger-scale and more varied soil environments, aiming to validate our current observations and assess the scalability and adaptability of the SoRo system for practical applications. We strongly believe that these will contribute to the development of more efficient and precise tools in the area of geotechnical engineering.

ACKNOWLEDGMENTS

The findings presented in this manuscript are based on work supported in part by the US National Science Foundation through PTE Federal Award No. EEC-1449501. Any opinions, findings, and conclusions or recommendations expressed in this material are those of the authors and do not necessarily reflect the views of the National Science Foundation. Additional funding was provided by the Elizabeth and Bill Higginbotham Professorship in the School of Civil Engineering at Georgia Tech.

REFERENCES

Borela, Rodrigo (2021). “Micromechanics of passive and active inclusions in granular media”. In.

Borela, Rodrigo et al. (2021). “Earthworm-inspired robotic locomotion in sand: an experimental study with X-ray tomography”. In: *Géotechnique Letters* 11.1, pp. 66–73.

Calderón, Ariel A et al. (2016). “Design, fabrication and control of a multi-material-multi-actuator soft robot inspired by burrowing worms”. In: *2016 IEEE international conference on robotics and biomimetics (ROBIO)*. IEEE, pp. 31–38.

Chen, Yuyan, Ali Khosravi, Martinez, and Jason DeJong (2021). “Modeling the self-penetration process of a bio-inspired probe in granular soils”. In: *Bioinspiration & Biomimetics* 16.4, p. 046012.

Chen, Yuyan, Ali Khosravi, Martinez, Jason DeJong, and Dan Wilson (2020). “Analysis of the self-penetration process of a bio-inspired in situ testing probe”. In: *Geo-Congress 2020*. American Society of Civil Engineers Reston, VA, pp. 224–232.

Chen, Yuyan and Martinez (2022). “Discrete element modeling of the anchor-tip interactions during self-penetration of a bio-inspired probe”. In: *Proceedings of the 20th International Conference on Soil Mechanics and Geotechnical Engineering*.

Chen, Yuyan, Martinez, and Jason DeJong (2024). “DEM simulations of a bio-inspired site characterization probe with two anchors”. In: *Acta Geotechnica* 19.3, pp. 1495–1515.

Das, R et al. (n.d.). *An earthworm-like modular soft robot for locomotion in multi-terrain environments. Sci Rep. 13, 1571 (2023)*.

He, Jia and Jian Chu (2014). “Undrained responses of microbially desaturated sand under monotonic loading”. In: *Journal of Geotechnical and Geoenvironmental Engineering* 140.5, p. 04014003.

Heung, HoLam, Philip WY Chiu, and Zheng Li (2016). "Design and prototyping of a soft earthworm-like robot targeted for GI tract inspection". In: *2016 IEEE international conference on robotics and biomimetics (ROBIO)*. IEEE, pp. 497–502.

Huang, Sichuan and Junliang Tao (2020). "Modeling clam-inspired burrowing in dry sand using cavity expansion theory and DEM". In: *Acta Geotechnica* 15.8, pp. 2305–2326.

Johnson, Don H (2006). "Signal-to-noise ratio". In: *Scholarpedia* 1.12, p. 2088.

Kamata, Masashi et al. (2018). "Morphological change in peristaltic crawling motion of a narrow pipe inspection robot inspired by earthworm's locomotion". In: *Advanced Robotics* 32.7, pp. 386–397.

Kim, Jongheon et al. (2018). "Development of a mole-like drilling robot system for shallow drilling". In: *IEEE Access* 6, pp. 76454–76463.

Kubota, Takashi et al. (2007). "Earth-worm typed drilling robot for subsurface planetary exploration". In: *2007 IEEE international conference on robotics and biomimetics (ROBIO)*. IEEE, pp. 1394–1399.

Laschi, Cecilia et al. (2009). "Design of a biomimetic robotic octopus arm". In: *Bioinspiration & biomimetics* 4.1, p. 015006.

Lee, Junseok, Hyunjun Lim, et al. (2019). "Concept design for mole-like excavate robot and its localization method". In: *2019 7th International Conference on Robot Intelligence Technology and Applications (RiTA)*. IEEE, pp. 56–60.

Lee, Junseok, Christian Tirtawardhana, and Hyun Myung (2020). "Development and analysis of digging and soil removing mechanisms for mole-bot: Bio-inspired mole-like drilling robot". In: *2020 IEEE/RSJ International Conference on Intelligent Robots and Systems (IROS)*. IEEE, pp. 7792–7799.

Lin, Huai-Ti, Gary G Leisk, and Barry Trimmer (2011). "GoQBot: a caterpillar-inspired soft-bodied rolling robot". In: *Bioinspiration & biomimetics* 6.2, p. 026007.

Luo, Yudong et al. (2016). "Scissor mechanisms enabled compliant modular earthworm-like robot: Segmental muscle-mimetic design, prototyping and locomotion performance validation". In: *2016 IEEE International Conference on Robotics and Biomimetics (ROBIO)*. IEEE, pp. 2020–2025.

Martinez, A et al. (2018). "Monotonic and cyclic centrifuge testing of snake skin-inspired piles". In: *Proceedings of biomediated and bioinspired geotechnics conference*.

Martinez et al. (2022). "Bio-inspired geotechnical engineering: principles, current work, opportunities and challenges". In: *Géotechnique* 72.8, pp. 687–705.

Naziri, Saeedeh et al. (2024). "Earthworm-inspired subsurface penetration probe for landed planetary exploration". In: *Acta Geotechnica* 19.3, pp. 1267–1274.

Niu, Sanku et al. (2015). "Enabling earthworm-like soft robot development using bioinspired IPMC-scissor lift actuation structures: Design, locomotion simulation and experimental validation". In: *2015 IEEE International Conference on Robotics and Biomimetics (ROBIO)*. IEEE, pp. 499–504.

Zhang, Ningning et al. (2023). "A bioinspired self-burrowing probe in shallow granular materials". In: *Journal of Geotechnical and Geoenvironmental Engineering* 149.9, p. 04023073.